

## A study of crystallization kinetics in semiconducting glassy alloy $\text{Cu}_{0.10}\text{As}_{0.45}\text{Te}_{0.45}$

C. Wagner, J. Vázquez, P. Villares and R. Jiménez-Garay

*Facultad de Ciencias, Universidad de Cádiz, Apartado 40, Puerto Real (Cádiz, Spain.)*

(Received September 22, 1993; accepted January 5, 1994)

### Abstract

A study of the crystallization kinetics of glassy alloy  $\text{Cu}_{0.10}\text{As}_{0.45}\text{Te}_{0.45}$  was made using a method in which the crystallization rate is deduced bearing in mind the dependence of the reaction rate constant on time, through temperature. The method was applied to the experimental data obtained by differential scanning calorimetry, using continuous-heating techniques. The alloy studied exhibited overlapping exothermic peaks which were resolved using a numerical method developed by the authors, making it possible to study the crystallization phases separately. The kinetic parameters determined have made it possible to discuss the different types of nucleation and crystal growth exhibited by each stage of crystallization process. The phases at which the alloy crystallizes after the thermal process have been identified by X-ray diffraction. In first stage of process, microcrystallites of AsTe are crystallized in an amorphous matrix. In the second transformation,  $\text{As}_2\text{Te}_3$  is crystallized. Finally, in the third stage the crystalline phase CuTe appear, coexisting with the aforementioned crystalline compounds.

### 1. Introduction

Traditionally, solid-state physics has meant crystal physics. Solidity and crystallinity are considered as synonymous in the texts on condensed matter. Yet, one of the most active fields of solid-state research in recent years has been the study of solids that are not crystals, solids in which the arrangement of the atoms lacks the slightest vestige of long-range order. The advances that have been made in the physics and chemistry of these materials, which are known as amorphous solids or as glasses, have been widely appreciated within the research community. Glassy alloys of chalcogen elements were the initial object of study because of their interesting semiconducting properties [1] and more recent importance in optical recording [2]. Recording materials must be stable in the amorphous state at low temperature and have a short crystallization time. Tellurium alloy films, in particular, are used as recording media as they have a low melting temperature and high absorption coefficients for the wavelengths of semiconducting lasers; promising materials with these characteristics have recently been studied [3, 4]. Glassy materials exhibit a characteristic transition temperature [5] from the more energetic glass phase to the minimal energy crystalline phase.

The study of crystallization kinetics in amorphous materials by differential scanning calorimetry (DSC) methods has been widely discussed in the literature [6–9]. There is a large variety of theoretical models and theoretical functions proposed to explain the crystallization kinetics. The application of each of them depends on the type of amorphous material studied and how it was made. For chalcogenide glasses obtained in bulk form, which is the case of the alloy  $\text{Cu}_{0.10}\text{As}_{0.45}\text{Te}_{0.45}$  we studied [10], the most adequate theoretical model turned out to be the so-called Johnson-Mehl-Avrami (JMA) model, which, although developed for isothermal processes, can be applied, under certain conditions, to continuous heating experiments [9], thus obtaining satisfactory kinetic parameters (activation energy,  $E$ , reaction order,  $n$ , and frequency factor,  $K_0$ ) for describing the crystallization reactions.

The present paper studies the crystallization kinetic of glassy alloy  $\text{Cu}_{0.10}\text{As}_{0.45}\text{Te}_{0.45}$ , which is characterized by aforementioned parameters, using differential scanning calorimetry with continuous-heating techniques. Finally, three crystalline phases corresponding to different stages of the exothermic reactions were identified by X-ray diffraction (XRD) measurements, using  $\text{CuK}\alpha$  radiation.

## 2. Theoretical background

### 2.1. Kinetic parameters

The theoretical basis for the interpretation of the DSC results is provided by the formal theory of transformation kinetics, as developed by Johnson, Mehl and Avrami [11–13]. In its basic form, the theory describes the evolution over time of the crystallized fraction,  $x$ , in terms of the nucleation frequency per unit volume,  $I_v$ , and the crystalline growth rate,  $u$ ,

$$x = 1 - \exp\left[-g \int_0^t I_v \left(\int_0^{\tau} u d\tau\right)^m dt\right] \quad (1)$$

where  $g$  is a geometric factor which depends on the shape of the crystalline growth and  $m$  is a parameter which depends on the mechanisms of growth and the dimensionality of the crystal. For the important case of isothermal crystallization with time-independent nucleation and growth rates, eqn.(1) can be integrated to obtain

$$x = 1 - \exp(-g' I_v u^m t^n) \quad (2)$$

where  $n=m+1$  for  $I_v \neq 0$  and  $g'$  is a new shape factor. Expression (2) can be identified with the Johnson-Mehl-Avrami relationship

$$x = 1 - \exp[-(Kt)^n] \quad (3)$$

in which  $K$  is defined as the reaction rate constant, which is usually assigned an Arrhenian temperature dependence

$$K = K_0 e^{-E/RT} \quad (4)$$

where  $E$  is the effective activation energy which describes the overall crystallization process and  $K_0$  is the frequency factor. Comparison of eqns. (2) and (3) shows that  $K^n$  is proportional to  $I_v u^m$  and, therefore, the consideration of an Arrhenian temperature dependence for  $K$  is only valid when  $I_v$ , and  $u$  vary with temperature in an Arrhenian manner.

In general, nucleation frequency and crystalline growth rate exhibit far from Arrhenius-type behaviour [14, 15]; however, for a sufficiently limited temperature range, such as the range of crystallization peaks in DSC experiments, both magnitudes can be considered to exhibit said behaviour.

It is a well-known fact that eqns. (3) and (4) are used as the basis of nearly all differential thermal analysis

(DTA) and DSC crystallization experiments, but it must be noted that expression (3) can only be applied accurately in experiments carried out under isothermal conditions, for which it was deduced. However, this expression is often used for deducing relationships describing non-isothermal crystallization processes, because the values obtained for kinetic parameters are in good agreement with those determined through other methods. In spite of this, it is more accurate to integrate eqn. (1) under non-isothermal conditions and to consider that both  $I_v$  and  $u$  have an Arrhenian temperature dependence, resulting in an expression like eqn. (3), as proved by de Bruijn et al. [16]. From this point of view, the crystallization rate is obtained by deriving expression (3) with respect to time, bearing in mind the fact that, in the non-isothermal process, the reaction rate constant is a time function through its Arrhenian temperature dependence [17], resulting in

$$\frac{dx}{dt} = n(Kt)^{n-1} \left[ t \frac{dK}{dt} + K \right] (1-x) \quad (5)$$

The maximum crystallization rate is found by making  $d^2x/dt^2 = 0$ , thus obtaining the relationship

$$[n-1-n(Kt)^n] \left( t \frac{dK}{dt} + K \right)^2 + Kt \left( 2 \frac{dK}{dt} + t \frac{d^2K}{dt^2} \right) = 0 \quad (6)$$

in which by substituting  $dK/dt$  and  $d^2K/dt^2$  for their expressions, introducing the heating rate  $\beta = dT/dt$  and considering  $T = T_0 + \beta t$  ( $T_0$  being the initial temperature), we obtain the expression

$$\begin{aligned} & \left( \frac{K_p (T_p - T_0)^n}{\beta} \right) \\ & = 1 - \frac{1}{n} \left[ 1 + \frac{2E}{RT_p} \left( \frac{T_p - T_0}{T_p} \right)^2 \right] \left[ 1 + \frac{E}{RT_p^2} (T_p - T_0) \right]^{-2} \end{aligned} \quad (7)$$

which relates the kinetic crystallization parameters  $E$  and  $n$  to the magnitude values (denoted by subscript  $p$ ) that can be determined experimentally, and which correspond to the maximum crystallization rate. For most crystallization reactions one typically observes that,  $[(T_p - T_0)/T_p]^2 \ll 1$  and eqn. (7) becomes:

$$\left[ \frac{K_p (T_p - T_0)^n}{\beta} \right] \approx 1 - \frac{1}{n} \left[ 1 + \frac{E}{RT_p^2} (T_p - T_0) \right]^{-2} \quad (8)$$

expression that has been specified for two interesting approximations as follows:

(i) The case where the activation energy,  $E$ , of the process is much less than  $RT_p$ , in which case it is verified that

$$y_p = -\ln(1 - x_p) = \left[ \frac{K_p (T_p - T_o)^n}{\beta} \right] \approx \frac{n-1}{n} \quad (9)$$

which makes it possible to determine the reaction order,  $n$ , from the experimental value of the crystallized fraction,  $x_p$ , corresponding to the maximum crystallization rate. By taking logarithms in eqn. (9) we obtain

$$\ln \frac{T_p - T_o}{\beta y_p^{1/n}} = \frac{E}{R} \frac{1}{T_p} - \ln K_o \quad (10)$$

the equation of a straight line the slope of which gives the activation energy, and from the ordinate at the origin the frequency factor,  $K_o$ , is obtained.

(ii) If  $E \gg RT_p$ , the result obtained is

$$y_p = \left[ \frac{K_p (T_p - T_o)^n}{\beta} \right] \approx 1 \quad (11)$$

an expression from which it is deduced that the crystallized fraction for the maximum crystallization rate is 0.63, which, as may be observed is independent of the heating rate and the reaction order. The logarithmic form of eqn. (11) is

$$\ln \frac{T_p - T_o}{\beta} = \frac{E}{R} \frac{1}{T_p} - \ln K_o \quad (12)$$

a linear relationship which makes it possible to calculate parameters  $E$  and  $K_o$ . At the same time, if the relationship  $K_p(T_p - T_o)/\beta = 1$  is introduced into eqn. (5), we obtain

$$n = \frac{\left. \frac{dx}{dt} \right|_p RT_p^2}{0.37EK_p(T_p - T_o)} \quad (13)$$

which makes it possible to calculate the reaction order or kinetic exponent,  $n$ .

It should be noted that in non-isothermal crystallization experiments where the reaction rate constant may be considered to be temperature dependent according to the Arrhenius relationship, the aforementioned approximation is the most adequate, because in most crystallization reactions  $E/RT_p \gg 1$  (usually  $E/RT_p \geq 25$ ) [18].

## 2.2. Resolving the overlapping peaks

The complexity of the transformations which take

place in the solid phase often shows DSC registers exhibiting overlapped peaks, where one reaction is superimposed on another within a certain temperature interval. The separation of the contribution that each of the reactions supplies to the experimental data is necessary, in order to carry out a study of their kinetics. The main problem, when approaching the resolution of overlapping peaks, is finding a function capable of describing a single crystallization reaction. A relatively broad, though not complete analysis of cases such as some alloys of glassy systems: Cu-Ge-Te [19] and Sn-As-Se [20], quoted in the literature, seems to make it advisable to fit each experimental peak to the sum of two Gaussian functions defined by [21]

$$f(T) = a [H(T_p - T) e^{-b_1(T - T_p)^2} + H(T - T_p) e^{-b_2(T - T_p)^2}] \quad (14)$$

where  $a$ ,  $b_1$  and  $b_2$  are three parameters determined through fitting, by least squares, to the experimental function, being  $H(T_p - T)$  and  $H(T - T_p)$  forms of the Heaviside function. The constant  $T_p$  is the value of temperature at which the crystallization rate is maximum.

From this point of view, the resolution of various overlapping peaks is a question of numerical calculation, which is explained in detail in the literature [21], and used in this work to study the multiphase crystallization reactions exhibited by the alloy  $\text{Cu}_{0.10}\text{As}_{0.45}\text{Te}_{0.45}$ .

## 3. Experimental procedure

Bulk  $\text{Cu}_{0.10}\text{As}_{0.45}\text{Te}_{0.45}$  glass was prepared by the standard melt quenching method. High purity (99.999%) copper, arsenic and tellurium in appropriate atomic percent proportions were weighed (total 7 g per batch) into quartz glass ampoules. The contents were sealed under a vacuum of  $10^{-4}$  Torr, heated to  $900^\circ\text{C}$  for about 5 h and then quenched in ice water, which supplied the necessary cooling rate for obtaining the glass. The ampoules were continuously rotated in the furnace to homogenize the contents. The amorphous nature of the material was checked through a diffractometric X-ray scan, in a Siemens D500 diffractometer. Thermal behaviour was tested by using a Thermoflex differential scanning calorimeter by Rigaku Co. Temperature and energy calibrations of the instrument were performed using the well-known melting temperatures and melting enthalpies of high-purity tin, lead and indium supplied with the instrument. Powdered samples weighing about 20 mg were crimped (but not sealed) in an aluminum pan and scanned at room temperature through their  $T_g$  at different heating rates of 2, 4, 8, 16 and  $32 \text{ K min}^{-1}$ . An empty aluminum pan was used as reference, and in all cases a constant  $60 \text{ ml/min}$  flow

of He-55 was maintained in order to drag the gases emitted by the reaction, which are highly corrosive to the sensory equipment installed in the DSC furnace. The glass transition temperatures,  $T_g$ , were considered as a temperature corresponding to the intersection of the two linear portions adjoining the transition elbow in the DSC trace. The crystallization temperatures,  $T_p$ , were identified as those corresponding to the maximum of each peak. The initial temperatures,  $T_0$ , of the reactions were identified as the corresponding inflexions in the thermograms.

With the aim of investigating the phases at which the samples crystallize diffractograms of the material crystallized during the DSC were obtained. The experiments were performed with a Philips diffractometer (type PW 1830). The patterns were run with Cu as target and Ni as filter ( $\lambda = 1.542 \text{ \AA}$ ) at 40 KV and 40 mA, with a scanning speed of  $0.1^\circ \text{ s}^{-1}$ .

## 4. Results

### 4.1 Crystallization kinetics

The DSC registers give three crystallization overlapping peaks for studied alloy. Fig. 1 shows the experimental curve superimposed on the associated theoret-

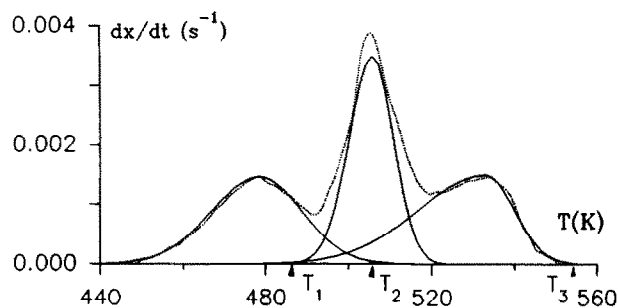


Fig. 1. Resolution of overlapping peaks through the associated theoretical functions representing them, for a heating rate of  $8 \text{ K min}^{-1}$  (— associated theoretical functions, ... experimental curve).

ical functions given by aforementioned numerical method, for a heating rate of  $8 \text{ K min}^{-1}$ . Table 1 shows the values obtained for parameters  $a$ ,  $b_1$ ,  $b_2$  and  $T_p$  [21] that make it possible to resolve the overlapping peaks of analyzed alloy, for each experimental heating rate. The crystallization kinetics in this case are studied, taking the data derived from the mentioned associated theoretical functions as the experimental data. Table 2 shows the characteristic temperatures of all the thermograms, as well as the enthalpies, for each stage of process calculated for different heating rates.

The area under the DSC curve is directly proportional to the total amount of alloy crystallized. The ratio between the ordinates and the total area of each peak gives the corresponding crystallization rates, which makes it possible to build the curves represented in Fig. 2 for each stage of crystallization process. It may be observed that the  $(dx/dt)_p$  values increase in the same proportion as the heating rate, a property which has been widely discussed in the literature [22], and which is less evident in the case of hard-to-solve multiple peaks.

Bearing in mind that, in most crystallization processes, the activation energy is much larger than the product  $RT$ , the crystallization kinetics of the alloy in question was studied according to the appropriate approximation, described in the preceding theory.

The plots of  $\ln [(T_p - T_0)/\beta]$  versus  $1/T_p$  at each heating rate and for all the stages of process, and also the straight regression lines carried out are shown in Fig. 3. From the slope of these experimental straight lines, according to expression (12), it is possible to deduce the values of the activation energy,  $E$ , for the crystallization processes studied. In addition, the origin ordinate of these straight lines gives the values corresponding to the frequency factors,  $K_0$ , which are given in Table 3 together with the activation energies.

By using the values of the frequency factor of the process, it is possible to calculate the value of the reaction rate constant,  $K_p$ , at each heating rate which corresponds to the maximum crystallization rate. The

TABLE 1. Parameters  $a$ ,  $b_1$ ,  $b_2$ ,  $T_p$  that make it possible to resolve the overlapping peaks of alloy  $\text{Cu}_{0.10}\text{As}_{0.45}\text{Te}_{0.45}$  for the different experimental heating rates.

$\beta$ ( $\text{K min}^{-1}$ )	1st stage				2nd stage				3rd stage			
	$10^3 a$ ( $\text{s}^{-1}$ )	$10^3 b_1$ ( $\text{K}^{-2}$ )	$10^3 b_2$ ( $\text{K}^{-2}$ )	$T_p$ (K)	$10^3 a$ ( $\text{s}^{-1}$ )	$10^3 b_1$ ( $\text{K}^{-2}$ )	$10^3 b_2$ ( $\text{K}^{-2}$ )	$T_p$ (K)	$10^3 a$ ( $\text{s}^{-1}$ )	$10^3 b_1$ ( $\text{K}^{-2}$ )	$10^3 b_2$ ( $\text{K}^{-2}$ )	$T_p$ (K)
2	0.433	6.023	4.337	469.3	1.082	13.202	10.880	496.1	0.390	3.450	5.262	514.5
4	0.692	4.528	5.597	475.9	2.100	10.480	9.881	501.8	0.916	3.638	1.505	524.5
8	1.447	5.638	7.284	478.5	3.682	2.298	3.079	505.8	1.476	2.853	1.563	533.1
16	2.983	7.739	13.234	485.4	4.680	42.254	20.262	511.7	2.201	3.781	20.232	544.7
32	5.659	4.955	6.441	492.6	9.301	11.814	8.860	518.8	4.778	1.949	33.403	557.4

TABLE 2. Initial peak temperature,  $T_o$ , maximum peak temperature,  $T_p$ , and calculated enthalpies, corresponding to the different experimental heating rates.

$\beta$ (K min <sup>-1</sup> )	Peak 1			Peak 2			Peak 3		
	$T_o$ (K)	$T_p$ (K)	$\Delta H$ (mcal mg <sup>-1</sup> )	$T_o$ (K)	$T_p$ (K)	$\Delta H$ (mcal mg <sup>-1</sup> )	$T_o$ (K)	$T_p$ (K)	$\Delta H$ (mcal mg <sup>-1</sup> )
2	443.0	469.3	4.14	479.0	496.1	6.23	484.0	514.5	2.96
4	446.9	475.9	3.24	482.2	501.8	6.76	486.2	524.5	3.86
8	452.8	478.5	4.51	486.1	505.8	5.34	489.1	533.1	4.93
16	456.9	485.4	3.85	489.9	511.7	5.54	492.9	544.7	4.10
32	463.3	492.6	4.75	492.6	518.8	5.88	495.6	557.4	4.29

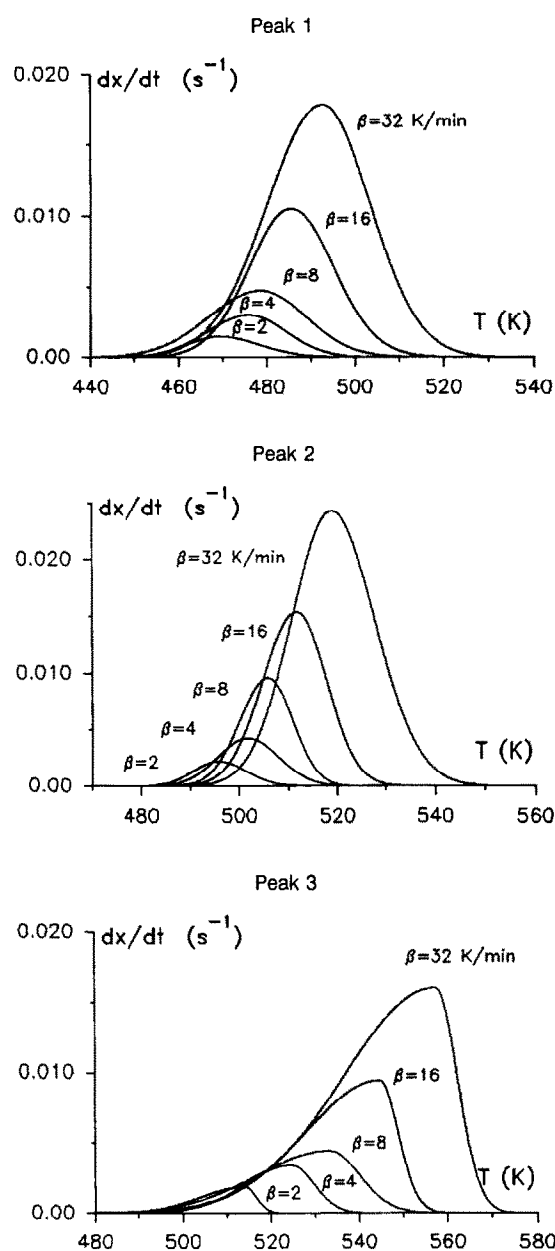


Fig. 2. Crystallization rate, versus temperature, found from the theoretical functions for each stage at different heating rates.

TABLE 3. The activation energies and frequency factors

Parameter	Peak 1	Peak 2	Peak 3
E (Kcal mol <sup>-1</sup> )	53.88	54.59	27.06
$K_o$ (s <sup>-1</sup> )	1.60·10 <sup>22</sup>	2.26·10 <sup>21</sup>	3.58·10 <sup>8</sup>

TABLE 4. The maximum crystallization rates, corresponding rate constants and kinetic exponents for the different heating rates.

Peak	$\beta$ (K min <sup>-1</sup> )	$10^3(dx/dt)_p$ (s <sup>-1</sup> )	$10^3K_p$ (s <sup>-1</sup> )	$10^3 \langle K_p \rangle$ (s <sup>-1</sup> )	n	$\langle n \rangle$
1	2	1.449	1.295	7.365	0.93	0.91
	4	2.996	2.885		0.81	
	8	4.738	3.932		1.07	
	16	10.532	8.800		0.99	
	32	17.856	19.991		0.75	
2	2	2.190	2.022	9.079	1.53	1.56
	4	4.213	3.792		1.40	
	8	9.598	5.846		2.09	
	16	15.400	10.936		1.66	
	32	24.289	22.798		1.08	
3	2	1.877	1.115	3.941	3.05	2.30
	4	3.388	1.900		2.53	
	8	4.430	2.888		1.96	
	16	9.422	4.987		2.15	
	32	16.002	8.814		1.81	

results for both magnitudes are shown in Table 4. These values make it possible to determine, through relationship (13), the reaction order,  $n$ , of each process corresponding to each one of the experimental heating rates. This parameter is also shown in Table 4, where the rate constant corresponding to the maximum may also be observed to exhibit a similar behaviour for the crystallization rate peak values, in relation to the heating rates.

According with the Avrami theory of nucleation, the relatively high values found for the frequency factor

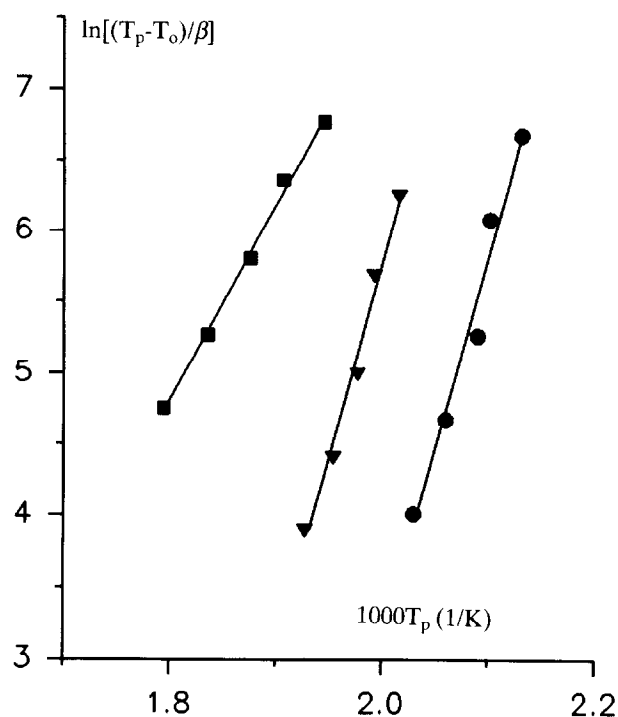


Fig. 3. Experimental plots and straight regression lines for all the peaks of the alloy  $\text{Cu}_{0.10}\text{As}_{0.45}\text{Te}_{0.45}$  ((•) peak 1, (▼) peak 2, (■) peak 3).

(related to the probability of molecular collisions) seem to confirm the fact that, in the crystallization reaction mechanism, there is a diffusion controlled growth, coherent with the basic formalism used.

Unambiguous conclusions on the crystalline growth morphology can only be deduced if, together with the thermal analysis carried out, direct techniques of Electron Microscopy are applied. However, in the absence of these, and using the usual criteria for the interpretation of reaction order [15, 23], some observations relating to the morphology of the growth can be worked out.

In glassy alloy  $\text{Cu}_{0.10}\text{As}_{0.45}\text{Te}_{0.45}$  there is a first very stable crystallization phase ( $E = 53.88$  Kcal/mol) exhibiting a surface nucleation mechanism. The second stage, which also is highly stable, has a high frequency factor, whereas the third, somewhat less stable, has a lower frequency factor. Calorimetric analysis is an indirect method which only makes it possible to obtain mean values for the parameters which control the kinetics of a reaction; however, as the reactions were virtually simultaneous, and the second shows high molecular agitation the aforementioned reaction conditions the third, even altering its nucleation mechanism. According with the literature [15] the second stage shows all shapes growing from small dimensions, zero nucleation rate, whereas the third stage exhibits a bulk crystallization mechanism with a decreasing nucleation rate.

#### 4.2 Identification of the crystalline phases

Taking into account the resolution of the overlapping peaks aforementioned of the glassy alloy  $\text{Cu}_{0.10}\text{As}_{0.45}\text{Te}_{0.45}$ , it is recommended to try to identify the possible phases that crystallize in each stage and coexist in the material after the overall crystallization by means of adequate DSC and XRD measurements. For this purpose the samples were heated at  $8 \text{ K min}^{-1}$  up to temperatures  $T_1$ ,  $T_2$  and  $T_3$ , shown in Fig. 1 and subsequently cooled to room temperature. The aforementioned temperatures were selected so as to avoid as much as possible interference of subsequent stages in the stage under consideration. The diffractograms corresponding to the samples heated at the three mentioned temperatures are shown in Fig. 4. Trace A of Fig. 4 has broad humps characteristic of the amorphous state of the starting material. The diffractograms of the transformed material during the first stage suggests predominance of the  $\text{AsTe}$  crystalline phase (indexed in trace B) and a small proportion of the  $\text{As}_2\text{Te}_3$  crystalline phase. In the second stage a consid-

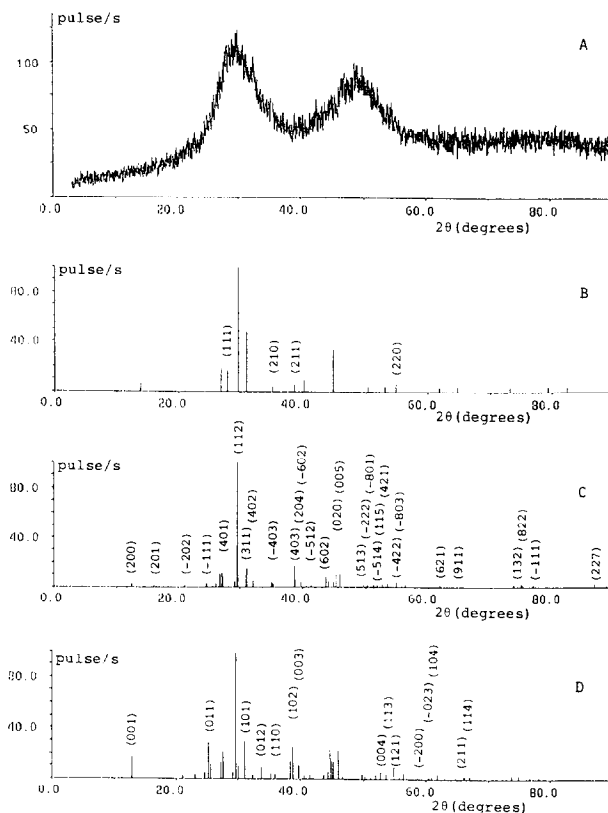


Fig. 4. Powder X-ray diffraction pattern for (A) as-quenched glass, (B) glass heated to the temperature  $T_1$  and cooled, (C) glass heated to the temperature  $T_2$  and cooled, and (D) glass heated past the three crystallization stage (temperature  $T_3$ ).

erable increase of the  $\text{As}_2\text{Te}_3$  crystalline phase (indexed in trace C) and a decrease of AsTe is observed which could be interpreted as a transformation of the latter substance into the first. Finally, the diffractogram of the samples heated to temperature  $T_3$  whose glassy material has already gone through the overall crystallization process is shown in Fig. 4D. One can observe the same crystalline peaks as in the previous stage together with those corresponding to the CuTe crystalline phase (indexed in trace D).

The found AsTe phase crystallizes in the cubic system [24] with the lattice parameter  $a = 5.778 \text{ \AA}$ , the  $\text{As}_2\text{Te}_3$  stoichiometric compound, shows monoclinic symmetry [25] with a cell unit defined by  $a = 14.339 \text{ \AA}$ ,  $b = 4.006 \text{ \AA}$ ,  $c = 9.873 \text{ \AA}$  and,  $\beta = 95^\circ$ . The CuTe crystalline phase detected in the third stage of the process shows symmetry orthorhombic [26] with the following parameters:  $a = 3.16 \text{ \AA}$ ,  $b = 4.08 \text{ \AA}$  and  $c = 6.93 \text{ \AA}$ .

The strong increase of the  $\text{As}_2\text{Te}_3$  crystalline phase together with the sharp drop of the AsTe crystalline phase in the last two stages of the crystallization process of the glassy alloy  $\text{Cu}_{0.10}\text{As}_{0.45}\text{Te}_{0.45}$  seems to suggest the existence of a transformation of the AsTe phase in the  $\text{As}_2\text{Te}_3$  phase throughout the mentioned process.

## 5. Conclusions

Crystallization of bulk  $\text{Cu}_{0.10}\text{As}_{0.45}\text{Te}_{0.45}$  glass has been studied using calorimetric and X-ray powder diffraction techniques. The study of crystallization kinetics was made using a method in which the crystallization rate is deduced bearing in mind the dependence of the reaction rate constant on time. This method for thermal analysis of glassy alloys proved to be efficient and accurate, giving results which were in good agreement with the nature of the alloy under study, which are representative of different nucleation and crystalline-growth processes, according to the values found for the reaction order. Identification of the crystalline phases were done by recording the X-ray diffraction patterns. In the first stage of process, microcrystallites of AsTe are crystallized in an amorphous matrix. In the second transformation,  $\text{As}_2\text{Te}_3$  is crystallized. Finally, in the third stage the crystalline phase CuTe appear, coexisting with the aforementioned crystalline compounds.

## Acknowledgments

The authors are grateful to the Junta de Andalucia and the Comision Interministerial de Ciencia y Tecnologia for financial support (Project No. MAT 92/0837).

## References

1. K. Tanaka, Y. Osaka, M. Sugi, S. Iizima and M. Kikuchi, *J. Non-Cryst. Solids*, 12 (1973) 100.
2. Y. Sugiyama, R. Chiba, S. Fugimori and N. Funakoski, *J. Non-Cryst. Solids*, 122 (1990) 83.
3. S. Fugimori, S. Sagi, H. Yamazaki and N. Funakoski, *J. Appl. Phys.*, 64 (1988) 100.
4. Y. Maeda, H. Andoh, I. Ikuta, M. Magai, Y. Katoh, H. Minemura, N. Tsuboi and Y. Satoh, *Appl. Phys. Lett.*, 54 (1989) 893.
5. S.R. Elliott, *Physics of Amorphous Materials*, Longman, Harlow, 1984.
6. H.E. Kissinger, *Anal. Chem.* 29 (1957) 1702.
7. D.J. Sarrach and J.P. De Neufville, *J. Non-Cryst. Solids*, 22 (1976) 245.
8. D.W. Henderson, *J. Non-Cryst. Solids*, 30 (1979) 301.
9. S. Surinach, M.D. Baró, M.T. Clavaguera-Mora and N. Clavaguera, *J. Non-Cryst. Solids*, 58 (1983) 209.
10. C. Wagner, J. Vázquez, P. Villares and R. Jimenez-Garay, *Mater. Lett.* 16 (1993) 243.
11. W.A. Johnson and K.F. Mehl, *Trans. Am. Inst. Mining Met. Eng.*, 135 (1981) 315.
12. M. Avrami, *J. Chem Phys.*, 7 (1939) 1103.
13. M. Avrami, *J. Chem. Phys.* 8 (1940) 212.
14. D. Turnbull, *Solid State Physics*, Vol. 3, Academic Press, New York, 1956.
15. J.W. Christian, *The Theory of Transformations in Metal and Alloys*, 2nd edn., Pergamon, New York, 1975.
16. T. J. W. de Bruijn, W.A. de Jong and P.J. van der Berg, *Thermochim. Acta*, 45 (1981) 315.
17. J.A. Augis and J.E. Bennett, *J. Thermal Anal.*, 13 (1978) 283.
18. H. Yinnon and D.R. Uhlmann, *J. Non-Cryst. Solids*, 54 (1983) 253.
19. R. A. Ligeró, J. Vázquez, M. Casas-Ruiz and R. Jiménez-Garay, *J. Thermal Anal.*, 39 (1993) 695.
20. C. Wagner, P. Villares, J. Vázquez and R. Jiménez-Garay, *Mater. Lett.* 15 (1993) 370.
21. C. Wagner, J. Vázquez, P. Villares and R. Jiménez-Garay, *Mater. Lett.* (to be published).
22. Y.Q. Gao, W.Wang, F.Q. Zheng and X. Liu, *J. Non-Cryst. Solids* 81 (1986) 135.
23. C.N.R. Rao and K.J. Rao, *Phase Transitions in Solids*, Mc Graw Hill, New York 1978.
24. M.F. Kotkata, A.M. Shamah, M.B. El-Den and M.K. El-Mously, *Acta Phys. Hung.* 54 (1983) 49.
25. G.J. Carron, *Acta Crystallogr.* 16 (1963) 338.
26. R.V. Baranova and Z.G. Pinsker, *Sov. Phys. Cryst.* 9 (1964) 83.